Received: 30 September 2022 | Revised: 5 April 2023 | Accepted: 7 May 2023

DOI: 10.1002/suco.202200949

ARTICLE

fib CEB-FIP WILEY

Combined effects of biochar and recycled plastic aggregates on mechanical behavior of concrete

Alice Sirico[1] | **Patrizia Bernardi**[1,2] | **Corrado Sciancalepore**[1,3] | **Beatrice Belletti**[1,2] | **Daniel Milanese**[1,2,3] | **Alessio Malcevschi**[2,4]

[1]Department of Engineering and Architecture, University of Parma, Parma, Italy

[2]Centre for Energy and Environment-CEE/CIDEA, University of Parma, Parma, Italy

[3]National Interuniversity Consortium of Materials Science and Technology (INSTM), Florence, Italy

[4]Department of Chemistry, Life Sciences and Environmental Sustainability, University of Parma, Parma, Italy

Correspondence
Patrizia Bernardi, Department of Engineering and Architecture, University of Parma, Parco Area delle Scienze, 181/A, Parma 43124, Italy.
Email: patrizia.bernardi@unipr.it

Funding information
Emilia Romagna Region, Grant/Award Number: PG/2018/632099

Abstract

Only in Europe, every year around 29 million tons of plastic waste are generated and only about 35% of such waste is collected for recycling. This results in huge amounts of plastic waste threatening the environment. One of the possible solutions for disposal can be represented by the concrete industry. Several research works have already studied the use of plastic waste in concrete mix as partial replacement for aggregates, showing that this use of plastics can contribute to reducing the environmental impact of concrete production by saving non-renewable resources. At the same time, lightweight concrete can be produced but at a non-negligible cost of a mechanical strength reduction. This work aims at investigating the effects on concrete physical and mechanical performances resulting from the introduction of recycled plastic aggregates in combination with another kind of waste used as filler, namely biochar. Biochar, which is the solid carbonaceous by-product resulting from wood-waste pyro-gasification, can have the role of carbon sequestrating additive in concrete, being able to fix carbon in a stable form in buildings for decades. The experimental findings obtained in this work show that the combination of biochar and recycled plastic waste, which was never investigated before, can help to obtain concretes with satisfactory mechanical performance, which promote circular economy principles. Thanks to biochar addition, the reduction in mechanical properties due to the presence of plastics is extremely limited with respect to control; moreover, these concretes demonstrate better behavior in terms of fracture energy and ductility.

KEYWORDS

biochar, circular concrete, fracture energy, mechanical characterization, recycled plastic aggregates, waste

1 | INTRODUCTION

The management of plastic waste and its recycling are nowadays topics of big concern. The global production of plastic has indeed increased from 15 million tons in 1964 to over 390 million tons in 2021 and it is expected to double in the next 20 years.[1] This means that the volume of plastics produced worldwide has grown more than 20-fold in the last decades, so making plastic the third man-made material most widely produced worldwide, after concrete and steel. Nowadays, every year, the post-consumer plastic waste collected in Europe amounts to about 29 Mt, of which about only 35% is recycled.[1] The production of plastics not only causes the exploitation of non-renewable natural resources, but the worst aspect is related to its disposal. Plastics need hundreds of years to degrade while releasing toxic pollutants into the environment.[2] When plastics are not dumped into landfills or recycled, they can be sent to energy recovery through incineration, which, however, results in carbon dioxide emissions, with the additional risk of releasing toxic compounds for the human health and the environment.[3] Due to the growing concerns about the environmental effects of post-consumer plastic waste disposal, the attainment of a higher recycling rate of plastic waste has become, in recent years, one of the major EU priorities. This goal implied the launch in 2015 of an EU Action Plan for circular economy and the consequent adoption of a Plastic Strategy in 2018,[4,5] with the aim of ensuring that all plastic packaging is reusable or easily recyclable by 2030.

The need for innovative solutions for plastic recycling has brought attention to the reuse of plastic waste in construction materials. The building industry is responsible for several negative impacts on the environment, particularly due to the production of cement-based materials, since only cement production, which exceeds 4 billion tons every year in the world, accounts for about 8%–10% of the global loading of carbon dioxide into the atmosphere.[6] Ordinary concrete typically contains 12% cement and 80% aggregate by mass.[7] Considering that worldwide over 30 billion tons of concrete are being produced each year,[8] this implies that concrete-making contributes not only to greenhouse gas emissions (from 4% to 8% of the world's CO_2) but also consumes a significant amount of natural resources. Sand, gravel, and crushed rock are used for concrete at the rate of more than 25 billion tons every year, adversely affecting the landscape, the riverbeds, and more in general ecosystems. Moreover, the mining, processing, and transport operations of aggregates consume considerable amounts of energy.

During the last decades, the use of different kinds of waste was attempted in concrete, with the dual aim of reducing the abovementioned environmental impacts and at the same time solving the solid waste disposal problem. Recycling of some materials, such as plastics, glass, and construction and demolition waste, allows for saving non-renewable resources by partially replacing natural aggregates,[9,10] while other secondary materials are used for reducing the emissions of greenhouse gases related to concrete production.[11] Among these latter, recent research developments have concerned the use of biochar as an alternative way to reduce the carbon footprint of cement-based materials.[12–15] Biochar is the solid by-product resulting from biomass pyrolysis or gasification, that is, processes of thermo-chemical conversion under controlled conditions aimed at obtaining energy, in the form of syngas. The solid waste of this process is biochar, a material that is nowadays used for a wide range of applications, mainly related to the agricultural field. However, it is often still disposed of in landfills. The use of biochar in construction materials not only means wise waste management, but it is also a strategy for storing carbon in the built environment. During pyrolysis, biochar particles capture a high volume of stable carbon in their chemical structure, and this means that carbon can be indirectly locked for decades in buildings, which become carbon-sink themselves. Moreover, when used in proper percentages as filler, biochar can enhance the mechanical properties of cement-based materials, such as compressive strength, flexural strength, and toughness.[16–25] These positive effects, strictly depend on the percentage of biochar addition, on its physical and chemical properties, as well as on the curing type and time adopted for the cementitious material. More in detail, improved performance can be observed for biochar additions between 1% and 5% (by weight of cement). This effect is mainly related to the ability of biochar particles to fill the voids as well as to retain mixing water and gradually release it with time, so promoting the development of hydration reactions, especially in case of long air curing.

Within the context of waste recycling and producing more sustainable concrete, this work aims at studying the effects on concrete mechanical performances related to the addition of biochar together with the partial substitution of natural aggregates with plastic waste. The recycling of plastics into concrete was deeply studied in past years since it can be seen as an ideal method for disposing of this kind of waste, giving rise to both economic and ecological advantages. This use of plastic waste can prevent the degradation of plastic in the environment by locking it into concrete, so reducing pollution. Moreover, the replacement of sand/gravel needed for concrete production with recycled plastics allows for reducing the environmental impact by decreasing energy consumption and saving virgin construction

TABLE 1 Sieve analysis of aggregates, in terms of cumulated sieve passing percentage (%) versus squared mesh size (mm).

	Cumulated sieve passing (%)	
Squared mesh size (mm)	**Sand**	**Gravel**
10.00	100.00	100.00
8.000	100.00	83.98
5.600	100.00	19.25
4.000	98.90	2.78
2.000	81.80	1.22
1.000	63.40	1.02
0.500	40.70	0.43
0.250	14.50	0.24
0.125	3.30	0.04
0.063	0.91	0.00

materials. Plastic waste can also be seen as a lightweight aggregate, reducing concrete density. However, several experimental studies on different kinds of plastic waste[26–29] demonstrated that the use of recycled plastic in partial replacement of aggregates generally tends to worsen concrete mechanical performances. This effect is mainly related to the chemical incompatibility between the plastic waste aggregates and the cement paste, being plastic hydrophobic and with a lower elastic modulus if compared to natural aggregates. Moreover, special attention should be paid during concrete production to avoid segregation, since, due to different densities, while plastic waste aggregates tend to float in the cement paste, natural aggregates sink.[30,31]

With this background, this research work aims at developing a circular concrete containing two completely different kinds of waste, namely biochar (from wood waste pyro-gasification) and plastics (from waste of industrial processes), able to give different but offsetting effects on concrete, in the context of carbon sequestration strategy, circular economy, and waste recycling. More in detail, the main idea behind the research is to promote the recycling of plastic waste into concrete while minimizing its negative effects on mechanical properties by adding biochar as filler, so to try to counterbalance the known reduction of strength related to the introduction of plastic. In the literature, both biochar and plastic have already been studied individually for possible use in concrete or cementitious materials, but no previous research has explored their combined use yet. The effect in the concrete of this combined use is herein assessed and discussed in terms of material microstructure, density, workability, water absorption, and mechanical properties.

TABLE 2 Physical properties of natural aggregates.

	Sand	Gravel
Particle density (g/cm^3)	2.646	2.640
Water absorption (%)	1.75	2.00

2 | MATERIALS

2.1 | Cement and natural aggregates

Since the main aim of the work was to study the effects of recycled plastic and biochar addition on concrete behavior, at first a standard concrete mix was assumed as a reference one, and then other mixes were defined by varying the percentages of waste addition.

For all the concrete mixes, Portland Limestone Cement Type II A-LL 42.5 R (characterized by a fineness of 3900 cm^2/g, as determined by the Blaine apparatus) was used.

As regards the aggregates, the grain size distributions of the calcareous sand and the siliceous gravel used in the experimentation, in terms of squared mesh size versus cumulated sieve passing are reported in Table 1. The particle density and the water absorption (defined as the water content of an aggregate in saturated but surface dry condition [SSD]), were determined according to EN 1097-6[32] and the results are reported in Table 2 for both sand and gravel.

2.2 | Plastic waste

Ecoplast Srl (Italy) provided regranulated plastic waste, which was composed of a mixture of low-density polyethylene (LDPE) and polyamide (PA), as shown in Figure 1a. This plastic waste derives from industrial processing and is generally disposed of in landfills, because of its composition variability ranging from 25 to 75 wt% of LDPE, making it difficult to reuse in mechanical re-processing. The production of post-production recycled plastic generally involves the following steps: transporting, sorting, grinding of plastic parts, separating, and packing of re-grinded plastic, which require a specific energy consumption of about 0.2–0.3 MJ/kg and a production of carbon dioxide equivalent (CO_2e) equal to 140–150 g CO_2e/kg.[33] However, the use of recycled plastic mitigates the environmental impact caused by the dispersion of non-degradable plastic in the environment and the depletion of natural resources for concrete production. Even if the chemical composition of the material may vary according to the various production batches, the

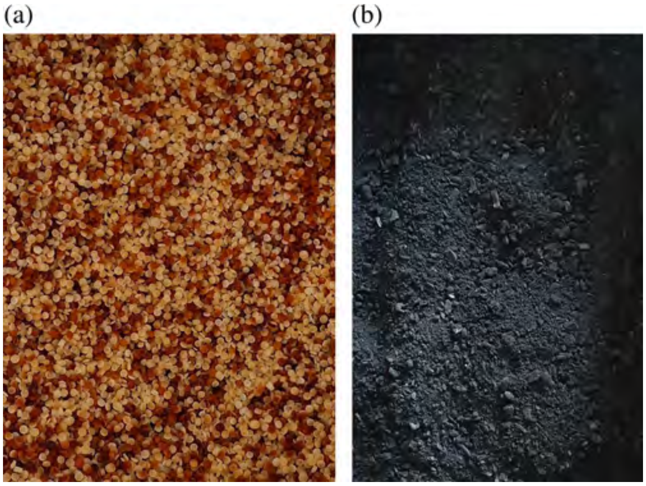

FIGURE 1 Waste materials used in the concrete mixes: (a) recycled plastic grains; (b) biochar.

overall characteristics of these recycled plastic grains change in a sufficiently narrow range to allow their use as a cement filler. Plastic grains were characterized by a uniform particle size distribution; each grain had smooth surfaces and a lentil shape with a base of 3–4 mm and a height of 1–2 mm.

2.2.1 | Infrared spectroscopy

Recycled plastic granules were analyzed by the infrared (IR) spectroscopy to determine their macromolecular structure. IR spectra were acquired using the Perkin-Elmer spectrum two FT-IR spectrophotometer, in attenuated total reflectance (ATR) mode with a diamond crystal plate. Each spectrum was the average of 16 scans, acquired in the range 4000–400 cm^{-1} and with a resolution of 4 cm^{-1}.

2.2.2 | Differential scanning calorimetry and thermogravimetry

The thermal parameters of recycled plastic grains, such as melting (T_m) and crystallization (T_c) temperatures, were obtained by differential scanning calorimetric (DSC) analysis. A small portion (10–20 mg) of the samples was subjected to DSC analysis using a Perkin Helmer DSC6000 (PerkinElmer). The heating scan was carried out in the thermal range 60/200°C with a rate of 10°C/min, while the cooling scan was set at a rate of 10°C/min from 200 to 0°C.

Thermogravimetry (TG) was used to verify the plastic thermal stability. In TG analysis (TGA 8000, Perkin Elmer) a plastic grain sample (about 10 mg) was heated from 30 to 900°C at a ramp of 10°C/min in N_2 atmosphere.

2.2.3 | Solid density

The plastic solid density is calculated by the helium pycnometer Ultrapyc 1200e (Quantachrome Instruments, Boynton Beach). About 6 g of powder was put in the small (10.8 cm^3) sample cell, and the density was expressed as the mean of 20 measurements.

2.3 | Biochar

The biochar used in this work (Figure 1b) is the carbonaceous by-product derived from an industrial downdraft fixed-bed pyro-gasification plant aimed at energy generation, located in the North of Italy. The incoming biomass is represented by woodchips, with dimensions between 30 and 90 mm and a moisture content of less than 8%. These woodchips are produced from locally sourced wood waste, mainly broadleaf trees.

To minimize the environmental impact, the biochar powder was used in the concrete mix as received from the plant, without any additional treatments, such as sieving or grinding. These two treatments, aimed at obtaining finer biochar particles, are energy-intensive processes that can reduce the benefit of inserting biochar into building materials to decrease the carbon footprint[34]; hence, it is better to avoid them, unless strictly necessary. In the present work, biochar was used as is, since previous research,[35] which used biochar coming from pyro-gasified wood waste as filler for cementitious materials, has shown that the advantages in terms of mechanical performance of these pre-treatments do not justify their use in terms of sustainability.

Biochar particles were physically and chemically characterized before being inserted as filler in the concrete mix. The biochar solid density value was calculated by the helium pycnometer Ultrapyc 1200e (Quantachrome Instruments, Boynton Beach). The particle size analysis was conducted in wet mode (i.e., employing water as dispersing medium) by using a laser granulometer (Mastersizer 3000, Malvern Instruments Ltd., Malvern) and the Fraunhofer approximation. The volume density in % was obtained as a function of the particle size in μm.

Scanning electron microscopy (SEM) images of biochar were collected by the field emission SEM (Nova NanoSEM 450, FEI company) using backscattered electrons for image acquisition.

TABLE 3 Mix proportions of batches in kg/m^3.

Mix	Cement	Fine aggregate	Coarse aggregate	Plastic	Biochar	Water	Plasticizer
C	408	1126	562	—	—	204	3.88
P13	408	900	562	74	—	204	1.92
P20	408	900	449	111	—	204	1.47
BP13	408	900	562	74	20.4	204	4.69

The energy dispersive x-ray spectroscopy system (X-EDS) (QUANTAX-200, Bruker, Germany) was used to obtain the quantitative elemental composition of biochar.

3 | EXPERIMENTAL PROGRAM

3.1 | Mix design and specimen preparation

The experimental campaign consisted of four concrete mixes: a reference concrete for control (named C), which is representative of a standard mix for concrete devoted to classical in situ applications, two concrete mixes containing an increasing percentage of recycled plastic granules (named P13 and P20), and a concrete mix with both biochar and plastic grains (named BP13). The numbers in the name of the batches stand for the percentage of substitution of traditional with recycled plastic aggregates.

The mix proportions of all the batches are reported in Table 3, so following a standard recipe for concrete (cement, sand, coarse aggregates, water, and plasticizer). The water-to-cement ratio was kept equal to 0.5 for all the mixes, while the percentage of aggregate substitution was varied. Due to the difference in specific gravity between natural and plastic aggregates, the volumetric design method was adopted: sand/gravel were partially substituted by plastic waste as a percentage by volume. Recycled plastic grains were added in substitution of 13% (for P13 and PB13 mix) or 20% (for P20 mix) of traditional aggregates. Natural aggregate proportions reported in Table 3 refer to SSD condition, so as recycled plastic grains, which were considered to be in a state of 0% absorption.

Additionally, starting from the mix proportion of P13, the batch named BP13 was obtained by adding biochar as a filler, at 5% by weight of cement. This percentage was chosen based on previous experimental findings obtained in Ref. 16 for structural concrete, since it combines a high recycling rate and carbon storage with enhanced mechanical properties.

All the mixes were prepared to obtain a homogeneous mixture without segregation and avoid the floatation of plastic grains on the concrete surface. At first, all the aggregates (both natural and recycled) were mixed for about 5 min with half of the required water in a drum-type mixer. Then, the cement and a quarter of the total water were added and mixed for 3 min. Finally, an acrylic-based superplasticizer and the remaining water were added, and the mixing continued for the last 4 min.

It is worth noticing that the addition of biochar requires a slight modification in the mixing sequence. As suggested in Refs. 16,22, biochar was previously pre-soaked for about 48 h before mixing, by immersing it in about 25% of the water computed for the mix design. This process was done to make biochar particles reach their saturation point, so to exploit the ability of biochar of retaining mixing water and gradually release it with time, promoting cement hydration. Then, the mixing sequence was the same adopted for the other batches: biochar was added in the first stage, together with the aggregates and 50% of the water required by the mix design, considering that 25% of the total water was already contained in biochar particles.

For each concrete mix, cylinders (100 × 200 mm^2, $d_c \times h_c$), cubes (150 × 150 × 150 mm^3), and prismatic specimens (100 × 100 × 400 mm^3) were cast to perform splitting, compressive and flexural tests, respectively. Moreover, additional cubes for density and water absorption measurements were prepared.

The cylindrical and cubic specimens were cast through three layers, while beams through two layers, and then compacted by using a vibrating needle. The specimens were covered with polyethylene sheets and demolded after 24 h. All the specimens devoted to the measurement of the mechanical performances were cured in water, while the cubes for density and water absorption measures were cured according to specifications of the regulation codes followed for test performing, that is, EN 12390-7[36] and ASTM C642-06,[37] respectively.

3.2 | Workability

Workability was evaluated through slump test according to EN 12350-2.[38] As can be seen from Table 3, the adopted superplasticizer dosage was different for each mix, since it was properly modified to obtain for all the

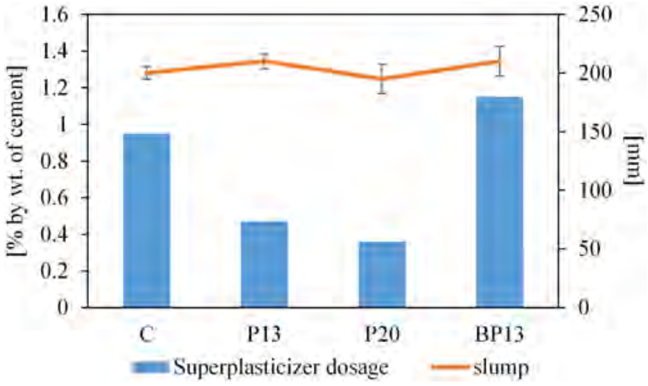

FIGURE 2 Required superplasticizer amount (% by wt of cement, left axis) and average slump values with the corresponding standard deviations (mm, right axis).

batches the same target consistency level, that was slump class S4 (160–210 mm), as defined by EN 206.[39] A typical amount of superplasticizer was chosen for control mix I, while a lower quantity was required for P13 and P20 mix, respectively equal to 50% and 62% less than that of control I, see Figure 2.

This effect is related to the non-absorptive characteristics and the hydrophobic nature of plastic grains, which lead to concrete mixes with more free water. A reduced amount of superplasticizer with respect to control means higher slump values if the amount of superplasticizer is maintained, which leads to obvious advantages for in situ applications, such as the possibility of obtaining good workability with lower water content.

On the contrary, to balance the loss of flowability due to biochar addition, 21% more superplasticizer was needed for BP13 samples. This effect is linked to the well-known ability of biochar particles to absorb water,[22] which considerably increases the amount of superplasticizer required, as already proved by past research.[13,17,21] This was also confirmed by the water absorption value of the used biochar, which was experimentally determined according to the method described in Ref. 40 and resulted equal to 2.08 ± 0.06 g of water per gram of biochar.

3.3 | Fresh and hardened density test

Fresh density was evaluated according to EN 12350-6,[41] after compacting the concretes with a vibrating needle. The density of hardened concrete was determined according to EN 12390-7[36] on three cubes for each mix, 28 days after demolding. The cubes were dried in a ventilated oven at 105 ± 5°C until their mass change of two successive measurements at intervals of 24 h was less than 0.2%.

3.4 | Water absorption test

The total amount of water absorption was determined by using the saturation method described in ASTM C642-06[37] on three cubes for each batch. At first, the oven-dried mass (*A*) of each cube was obtained by placing it in a ventilated oven at 105 ± 5°C until the measurement indicated approximately constant mass (i.e., mass changes by less than 0.5% in 24 h). Then, the saturated mass (*B*) of the samples was obtained by immersing them in water at approximately 20°C for not less than 48 h and until the mass change of each cube in the condition of dry surfaces was less than 0.5%. Then the water absorption was computed as $[(B–A)/A] \times 100$.

3.5 | Digital and scanning electron microscopy

To verify the distribution of the plastic grains and biochar particles in the concrete matrix, digital images of the samples were taken with a USB Digital Microscope (DM) equipped with the MicroCapture software. SEM was performed to obtain information on the interactions at the plastic/concrete and biochar/concrete interface. SEM characterizations were conducted with a field emission SEM (FESEM, Nova NanoSEM 450, FEI Company). Images were acquired in field-free lens mode making use of the circular backscatter detector (CBS). The accelerating voltage (HV) of 15 kV, the spot size of 4 a.u., and the working distance (WD) of about 6 mm were utilized in the acquisition of all images.

3.6 | Mechanical tests

Compressive tests were performed at 7 and 28 days of curing, in compliance with EN 12390-3,[42] by using a Universal Testing Machine METROCOM PV P30. The load was applied with a constant rate of 0.5 MPa/s and the measurements were carried out on three cubic samples for each concrete mix, at each time of curing.

The splitting tensile tests were performed by using the same Universal Testing Machine, following EN 12390-6[43] recommendations. A compressive force was increased continuously at a constant rate of 0.05 MPa/s along the length of each cylinder, which was placed horizontally between two parallel plates of the testing machine until the brittle failure of the specimen occurred.

Flexural tests were carried out according to JCI-S-001-2003,[44] by using a three-point bending (3 PB) loading scheme on beams characterized by a 2 mm wide and 30 mm deep notch at mid-span (Figure 3).

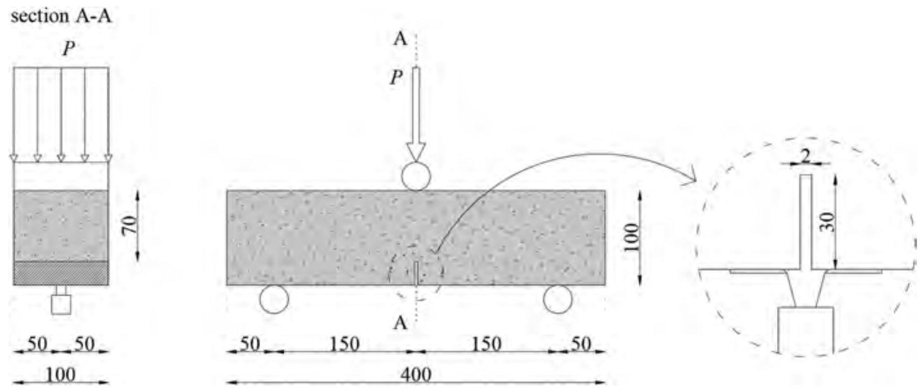

FIGURE 3 Testing configuration and geometry for three-point bending test (dimensions in mm) according to JCI-S-001-2003[44]: (a) midspan cross-section geometry of specimen; (b) longitudinal view; (c) detail of the beam notch and the clip gauge for CMOD control.

The tests were performed on four specimens for each mix, by means of a high-precision servo-electric Universal Testing Machine (INSTRON 8862), by controlling the crack mouth opening displacement (CMOD) with a clip-on strain gauge, and by measuring simultaneously the load. A speed of 0.6 mm/h was adopted at the beginning of the test to reach the peak load P_{max} in about 5 min; then, the speed was progressively increased until a residual load of about 0.015 kN was obtained.

Flexural strength σ_f and fracture energy G_f were evaluated for each specimen from the load *P–CMOD* response, according to Equations (1) and (2), respectively:

$$\sigma_f = P_{\max} \frac{3S}{2bh^2} \tag{1}$$

$$G_f = \frac{0.75W_0 + W_1}{A_{lig}} \tag{2}$$

where b and h (which are equal to 100 mm and 70 mm, respectively) are the width and net depth of the notched mid-cross section, while S is the net span, equal to 300 mm (Figure 3). It is worth noticing that the precise values of these quantities were carefully measured for each beam and then used for the calculation. Moreover, W_0 is the area under *P–CMOD* curve, W_1 is related to the work done by the deadweight of the specimen and the loading equipment, while A_{lig} is the area of the ligament (equal to $b \times h$).

4 | RESULTS AND DISCUSSION

4.1 | Plastic grain and biochar characterization

The IR spectra of the polymeric grains, in Figure 4, allow determining the main structural characteristics of the polymeric materials used, giving information on the possible interactions that can be created at the interface between polymer grains and cement. In the grains with higher concentration of PE, the characteristic IR peaks of this polyolefin can be identified in Figure 4a. The PE main stretching vibrations appear at 2916 cm^{-1} (asymmetric CH_2 stretch) and 2848 cm^{-1} (symmetric CH_2 stretch). The main bending modes of the CH_2 groups are located in the IR spectrum at 1471 and 1462 cm^{-1} (the CH_2 scissors vibration) and at 730 and 720 cm^{-1} (CH_2 rocking).[45] On the other hand, the spectrum of the PA-rich sample is shown in Figure 4b. The PA characteristics bands are at 3297 (the stretching of N—H group), 3078 (the first overtone of amide II), 2849 and 2918 cm^{-1} (respectively the symmetrical and asymmetrical stretching of CH_2). The band at 1637 cm^{-1} corresponds to the amide I absorption (stretching of the C=O + C—N groups) and the peak at 1541 cm^{-1} is due to the amide II vibration (N—H in plane bending + C—N stretching).[46]

The thermal characteristics, obtained by DSC, of the polymeric grains are shown in Figure 5. The melting and crystallization temperature, observed at 129 and 111°C, respectively (Figure 5a), are compatible with the characteristics of a regranulated low-density PE.[47] By considering a melting enthalpy (ΔH_m) of 102 J/g, the PE crystallinity degree—defined as $\%C = (\Delta H_m / \Delta H_m^0) \times 100$—can be assumed about equal to 35%. ΔH_m^0 is the melting enthalpy for a 100% crystalline polymer and it was taken as 293 J/g for PE.[48]

The DSC curve of the grains with the higher PA content is shown in Figure 5b. An additional melting peak during the heating scan is visible at approximately 210°C, while a crystallization peak at 170°C can be seen in the cooling scan. These temperatures are in line with the characteristic thermal behavior of a PA6.[49] With a melting enthalpy of about 30 J/g, the %C of the PA fraction was calculated at about 13%, by using literature data for the ΔH_m^0 ≈230 J/g of 100% crystalline PA6.[50]

From a thermal point of view, both types of recycled plastic grains (PE and PA rich samples) completely decomposed in a single degradative step around 500°C, as shown in Figure 6.

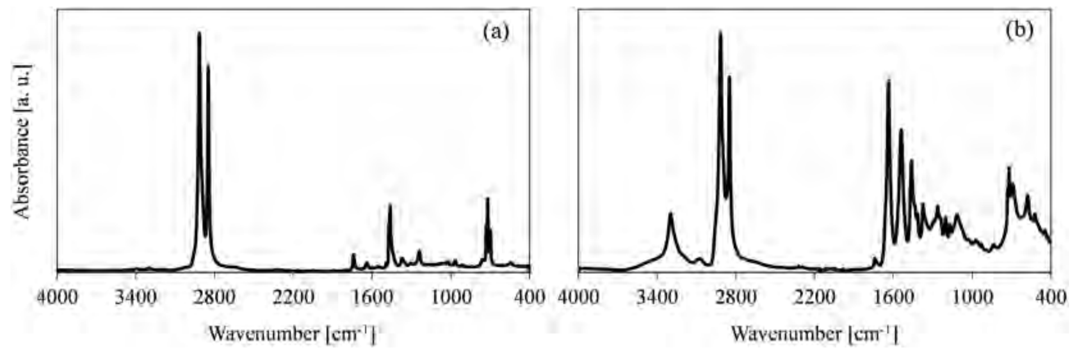

FIGURE 4 Infrared spectra of the granules rich in: (a) PE, and (b) PA; (a.u. arbitrary unit).

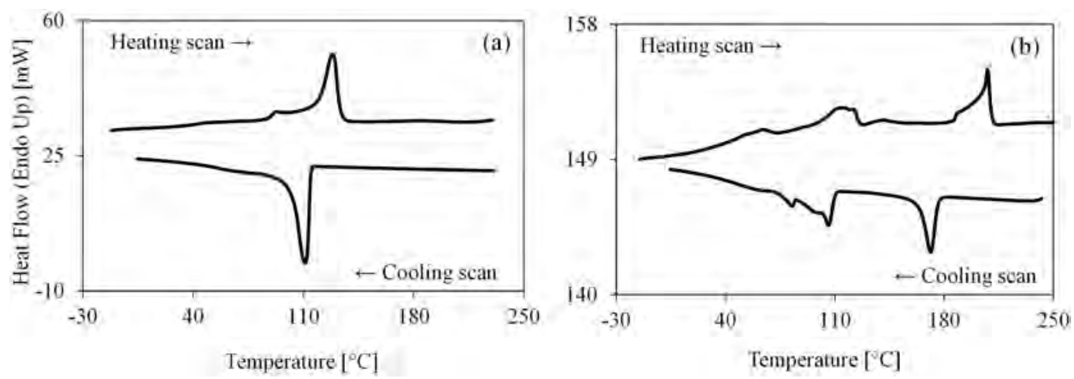

FIGURE 5 Differential scanning calorimetric curves of the granules rich in: (a) PE and (b) PA.

The mean plastic solid density, obtained by analyzing a random set of plastic grains as reported in Section 2.2.3, was 0.868 ± 0.001 g/cm^3, thus resulting significantly less than the corresponding one of natural aggregates (equal to 2.64 g/cm^3).

The physical characteristics of the biochar, useful for calculating the mix design, were obtained experimentally. The solid density value resulted equal to 2.04 ± 0.01 g/cm^3, a value in line with relatively high production temperatures typical of the pyro-gasification process and the type of feedstock.

As it appears from the particle size analysis (Figure 7a), the biochar particle distribution is relatively broad, with a span equal to 5.789. However, the volume-weighted mean DV-mean, equal to 236 ± 60 μm, and the standard percentiles of grain size D10, D50, and D90, equal respectively to 11, 107, and 634 μm, confirm the possible use of this biochar as filler for concrete production.

The broad dimensional distribution of the biochar is also confirmed by the SEM analysis (Figure 7b), which shows an extremely heterogeneous structure, in terms of size and composition. In fact, in addition to the carbon-based pyro-gasification residues, inorganic compounds are present in the system, as highlighted by the elemental compositions reported in Figure 7b.

4.2 | Concrete specimens with biochar and plastic grains

4.2.1 | Fresh and hardened density

The effect of the use of recycled plastic granules and biochar on density can be seen in Figure 8. By comparing the values obtained with those of the reference plain concrete mix (C), it can be observed that, as expected, the plastic grains lead to a reduction of density, with the same trend for both fresh and hardened values. Thanks to the low specific gravity of plastic grains with respect to natural aggregates, the density decreases for increasing values of substitution, leading to a maximum decrease of about 15% for P20 samples with 20% of aggregate substitution. The obtained density value allows classifying P13 and P20 as lightweight concrete of density class D2.0 (according to Eurocode 2[51] classification).

The addition of biochar (BP13 samples) determines a further slight reduction in density with respect to the corresponding mix with the same amount of plastic (i.e., P13). This result is probably related to the combination of two opposite effects. Concrete density tends to be reduced by the low density of biochar particles, which are characterized by high porosity, as highlighted

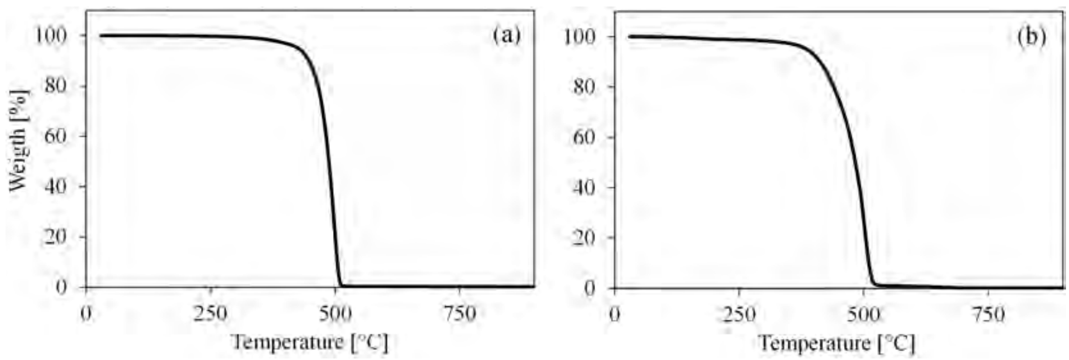

FIGURE 6 Thermogravimetry curves of the granules rich in: (a) PE and (b) PA.

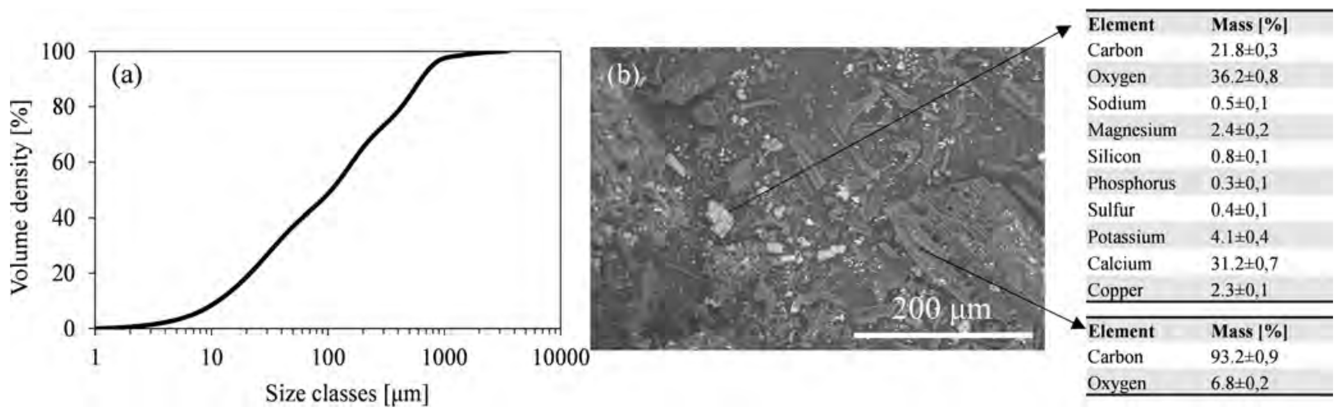

FIGURE 7 Biochar sample: (a) cumulative particle size distribution and (b) scanning electron microscopy image, with list of the elemental compositions of two characteristic points in the heterogeneous structure of biochar.

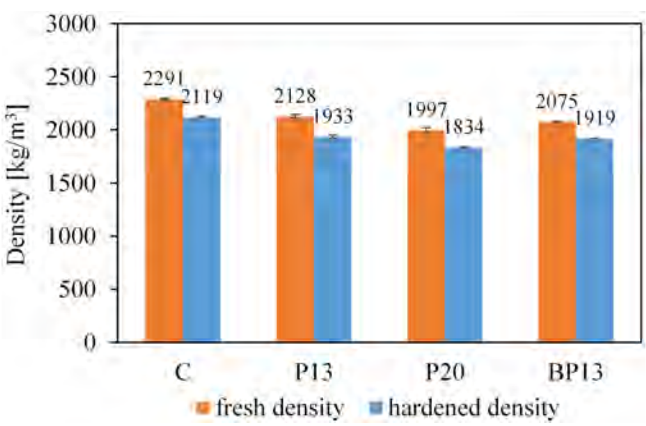

FIGURE 8 Average fresh and hardened density values with the corresponding standard deviations, for concrete mixes containing recycled plastic grains (P13 and P20) and containing both biochar and recycled plastic grains (BP13), compared to reference concrete (C).

in several works,[12,52,53] while an increase is related to the de-aerating and filler effects promoted by biochar, which is able to fill the voids, so reducing the porosity of the cement matrix.[16]

4.2.2 | Water absorption

The water absorption measurements for concretes with different amounts of plastic are reported in Table 4. Although the recycled plastic granules have a non-absorbent nature themselves, increasing substitution rates of natural aggregates with plastic grains lead to higher total water absorption values with respect to reference concrete (C). This effect is caused by the higher porosity of concretes containing plastics: the plastic grains, being hydrophobic, cannot chemically bind with the cement paste, leading to a highly porous interfacial transition zone between the recycled plastic granules and the cement paste. Anyway, absorption (%) is lower than 10% in all the mixes, which is the recommended limit for good quality cementitious mixes for practical applications.[54]

The ability of biochar particles to fill the voids, which enables the creation of a denser structure of concrete, contributes to the slight reduction of water absorption of BP13 with respect to the corresponding mix with the same amount of plastic, P13. Experimental findings in the literature[55] suggest that the addition of biochar at 1%–2% by weight of cement is effective in reducing the water absorption in cementitious mortars, but this fails for higher percentages. This is the reason why the addition of 5% by weight of cement used for concrete BP13 shows a slightly reduced value, but is almost comparable with that of P13.

TABLE 4 Water absorption results.

Mix	Water absorption (%)
C	8.20
P13	9.54
P20	9.86
BP13	9.42

4.2.3 | Microscopy analysis

Figure 9a,b report the DM images of samples C and BP13, respectively. The reference concrete and the biochar-plastic concrete samples do not show any considerable difference at this magnification. On the contrary, at higher magnifications, shown in the SEM images of Figure 9c,d, a different behavior of biochar and plastic grains, respectively, towards the cement matrix can be noted. At the biochar-cement interface, there is no phase separation: the two materials give life to a continuous and homogeneous microstructure due to the compatibility between the two components (Figure 9c). On the other hand, in the case of plastic grains, the formation of a separation layer is clearly observed between the hydrophobic polymer surface and the hydrophilic cement matrix, determining a microstructural discontinuity (Figure 9d).[56]

4.2.4 | Compressive strength

As can be seen in Figure 10, the average compressive strength decreases at both 7 and 28 days of curing, when recycled plastic granules are used in the concrete mix. An almost linear reduction can be observed as the percentage of substitution of natural aggregates increases from 0% of reference concrete (C), to 13% (P13) and 20% (P20). As can be further observed from Figure 11, the obtained experimental data suggest a linear relationship between density and compressive strength, so confirming the same correlation between these two variables already found in the literature for LDPE aggregates.[57]

The degradation of compressive strength when plastic grains are added to the concrete mix can be attributable to the following aspects. The physical–chemical incompatibility between the plastic grains, which are characterized by hydrophobic properties, and the cement matrix, which is substantially hydrophilic, causes the presence of not absorbed water, a reduced cement hydration reaction near the surface of the plastic grain as well as the presence of an empty interface between the two materials, as also observed by SEM (Figure 9d). This worsens the bond strength between the surface of the plastic grains and the cement matrix, and increases the porosity of the concrete, as highlighted also by the results of the water absorption test. Moreover, also the lower stiffness of recycled plastic granules with respect to natural aggregates plays an important role in reducing the compressive strength of the concrete.

The addition of 5% biochar (by weight of cement) is able to partially counterbalance the negative effects related to plastics. As a matter of fact, the mechanical behavior of concrete containing plastic improves when biochar is added to the mix (Figure 10), thanks to filler effects provided by finer biochar particles, as well as to their ability to absorb water. The voids due to plastic addition are partially filled by biochar as well as the water not absorbed by the plastic grains can be soaked up by biochar particles (Figure 12a). As a consequence, compressive strength improves, so obtaining an enhancement of about 20% by comparing BP13 and P13 values.

4.2.5 | Tensile strength

The partial replacement of natural aggregates with recycled plastic grains causes a decrease in splitting tensile strength, as can be seen in Figure 13, which reports the average experimental values at 28 days of curing with the related standard deviations. However, splitting tensile strength appears less affected than compressive strength by the use of plastic aggregates, as already stated in the literature for different kinds of plastic waste.[26] This effect can be better appreciated in Figure 14, which relates the experimental compressive strengths to splitting tensile strength values, obtained or as results of the experimental campaign or by applying the relations reported in Eurocode 2[51] for ordinary (section 3.1.2 in Ref. 51) and lightweight (section 11.3.1 in Ref. 51) concrete. It can be observed that Eurocode 2 relations for ordinary concrete, which provide a close correlation to the experimental value of reference concrete (C), underestimate the splitting tensile strength of P13 and P20 concrete mix. However, by applying the Eurocode 2 relations for lightweight concrete, the experimental and analytical values are almost coincident, meaning that the effect of recycled plastic grains on tensile behavior is comparable to that of ordinary not-recycled lightweight aggregates.

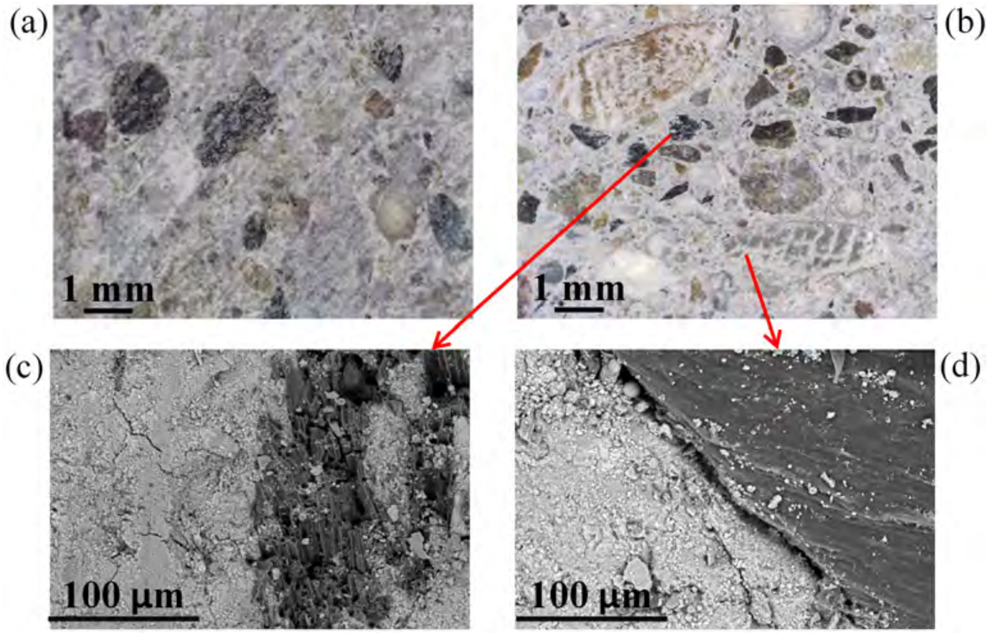

FIGURE 9 Digital microscopy images of: (a) C and (b) BP13 (b) samples. Scanning electron micrographs at the interface (c) biochar/cement matrix and (d) plastic grain/cement matrix.

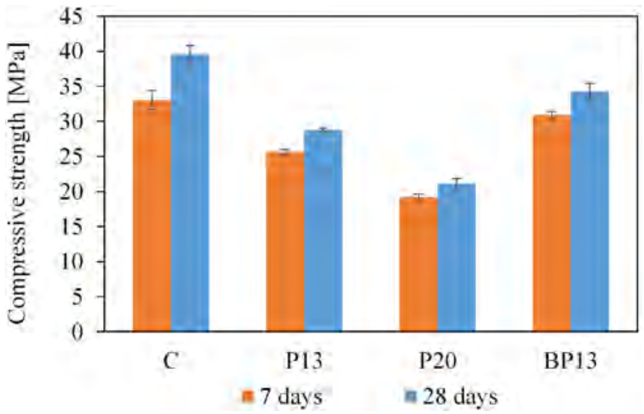

FIGURE 10 Average compressive strength with the corresponding standard deviation, for 7 and 28 days of curing, for concrete mixes containing recycled plastic grains (P13 and P20) and containing both biochar and plastic grains (BP13), compared to reference concrete (C).

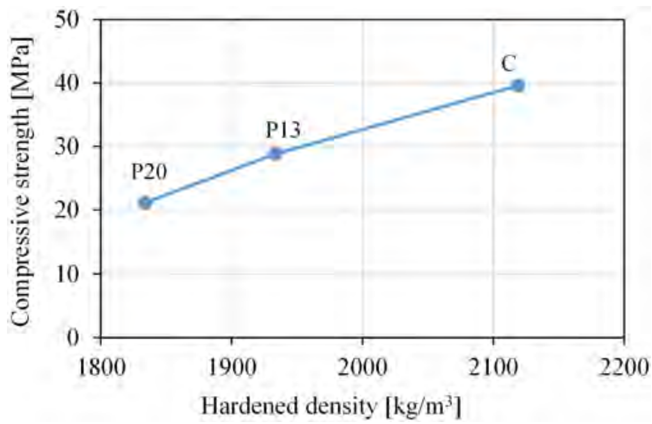

FIGURE 11 Correlation between hardened density and 28-days compressive strength for concrete mixes containing recycled plastic granules (P13 and P20) compared to reference concrete (C).

As can be seen from Figure 13, the presence of biochar (BP13) improves concrete tensile strength by only 2.5% with respect to concrete with the same amount of plastic but without biochar (P13). The higher capability of biochar particles of improving compressive rather than tensile behavior is known in the literature for cementitious composites (without plastic).[16,18,22,58] This effect is due to the presence of air voids in the tensile plane of concrete caused by biochar addition, as well as to the low strength of biochar particles. As known, cementitious materials are characterized by a brittle nature in tension, with micro-cracks that spread quickly and develop into macro-cracks, resulting in failure. Finer biochar particles acting as filler may help to control micro-cracking growth by filling the pores, thanks to the smaller size of biochar, compared to the other components in concrete. On the other hand, biochar particles, especially in the case of inhomogeneous particle sizes ranging to high values, can also agglomerate, so producing air voids. This can lead to a formation of a weaker interfacial zone, resulting in tensile strength values comparable (or even lower) with respect to concrete without biochar. Biochar particles used in this study are characterized by a relatively broad distribution with a maximum dimension of up to 3 mm (Figure 7), which tends to attract cracks during tensile tests. On the other hand, these defects are probably less critical during compressive tests because they tend to be closed during testing.

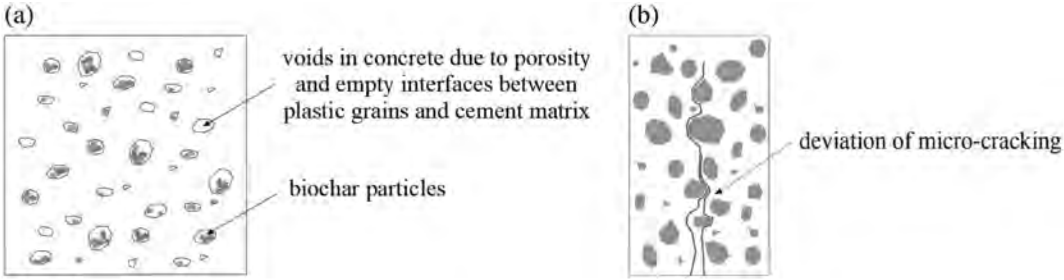

FIGURE 12 Scheme of mechanisms offered by biochar particles in concrete with plastic grains: (a) biochar filler effect and (b) tortuosity of micro-cracking due to biochar particles.

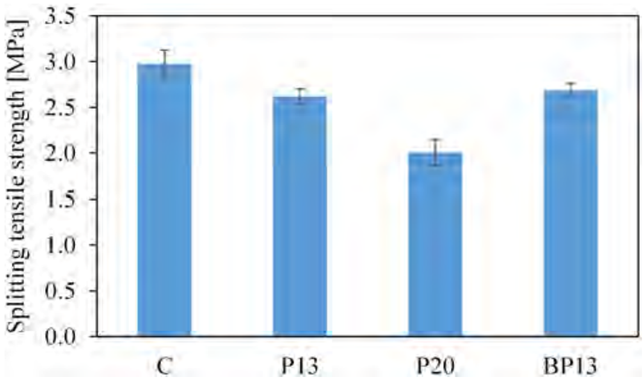

FIGURE 13 Average 28-days splitting tensile strength with the corresponding standard deviation, for concrete mixes containing recycled plastic grains (P13 and P20) and containing both biochar and plastic grains (BP13), compared to reference concrete (C).

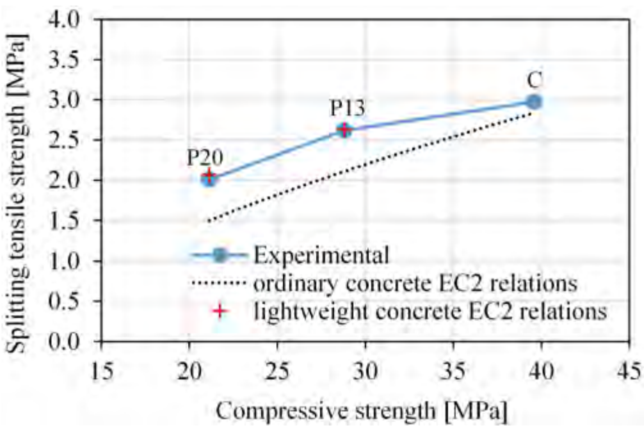

FIGURE 14 Experimental and theoretical (EC2) correlation between splitting and compressive strength for concrete mixes containing recycled plastic granules (P13 and P20) compared to reference concrete (C).

4.2.6 | Flexural strength and fracture energy

The less negative effects of recycled plastic aggregates on tensile with respect to compressive strength of concrete are also confirmed by the results of flexural tests, which are reported in Figure 15a in terms of peak stress. Even if for the highest percentage of aggregate substitution (P20) a decrease can be recognized with respect to reference concrete (C), when 13% of natural aggregates are substituted by plastic (P13), the average flexural strength at 28 days of curing is almost equal to that of C mix.

3 PB tests under CMOD control allow obtaining also the fracture energy, which is computed as the area under *P–CMOD* curve (Figure 16), and so measure the amount of energy absorbed until the sample breaks into two parts. In this case, recycled plastic aggregates provide significant increases in fracture energy, as shown in Figure 15b, where 30% and 95% higher values can be observed for P13 and P20 with respect to control (C) concrete, respectively. This happens thanks to the ability of plastic grains to slow down the propagation of micro-cracks, so obtaining concretes characterized by greater displacement at failure and higher residual loads in post-peak response (Figure 16).

To better analyze the post-cracking behavior, the residual flexural tensile strengths $f_{R,i}$ were evaluated for different values of $CMOD$ ($CMOD_1 = 0.5$ mm, $CMOD_2 = 1.5$ mm, $CMOD_3 = 2.5$ mm), according to Equation (3):

$$f_{R,i} = P_i \frac{3S}{2bh^2} \quad (3)$$

where P_i represents the load corresponding to $CMOD_i$.

The mean residual strengths $f_{R,1}$, $f_{R,2}$, $f_{R,3}$, and the corresponding standard deviations are reported in Table 5. For $CMOD_1 = 0.5$ mm, P13 and P20 mixes show an increase in the mean value of the residual strengths $f_{R,1}$ equal to 41% and 168%, with respect to control (C). Moreover, while C mix at $CMOD_1 = 0.5$ mm retains only 11% of its flexural strength, P13 and P20 maintain 16% and 47% of their peak stresses, respectively. So, as can be observed, concretes containing plastic are characterized by greater ductility and toughness with respect to control.

When biochar is added to the concrete mix (BP13), a reduction in flexural strength of about 20% with

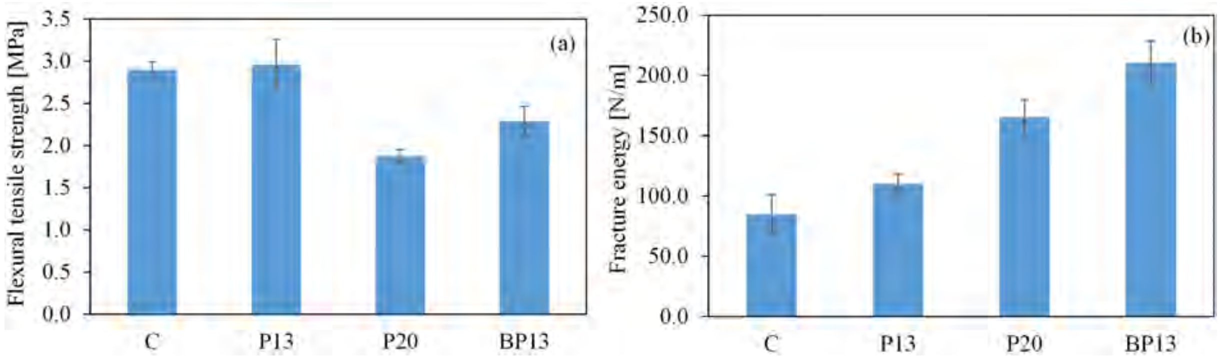

FIGURE 15 Average 28-days (a) flexural tensile strength and (b) fracture energy, with the corresponding standard deviation, for concrete mixes containing recycled plastic grains (P13 and P20) and containing both biochar and plastic grains (BP13), compared to reference concrete (c).

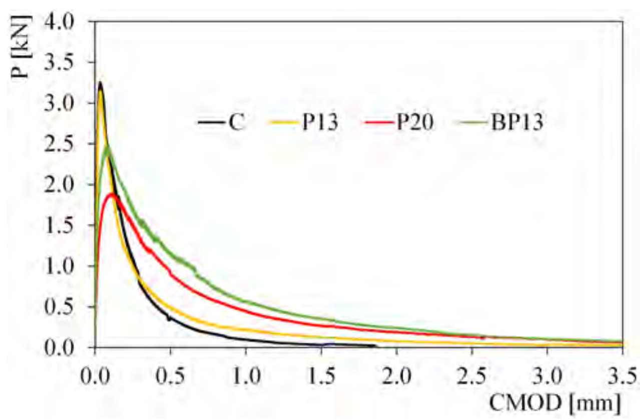

FIGURE 16 Average load *P* versus CMOD curves from three-point bending tests of concretes containing recycled plastic grains (P13 and P20) and containing both biochar and plastic grains (BP13), compared to reference concrete (C).

TABLE 5 Average residual strengths $f_{R,1}$, $f_{R,2}$, $f_{R,3}$, with the corresponding standard deviations for concrete mixes containing recycled plastic grains (P13 and P20) and containing both biochar and plastic grains (BP13), compared to reference concrete (C).

Mix	$f_{R,1}$ (MPa)	$f_{R,2}$ (MPa)	$f_{R,3}$ (MPa)
C	0.331 ± 0.119	—	—
P13	0.466 ± 0.067	0.119 ± 0.018	—
P20	0.887 ± 0.099	0.263 ± 0.028	0.131 ± 0.021
BP13	0.983 ± 0.215	0.313 ± 0.059	0.145 ± 0.015

respect to the corresponding mix without biochar (P13), can be recognized by analyzing Figure 15a. This can be attributed to a not optimal dispersion of biochar in the cement matrix and the formation of air voids in the tensile plane, as well as to the low strength of biochar particles, as already highlighted for splitting strength. However, the negative effect on flexural strength is largely counterbalanced by the considerable increase in fracture energy, whose value presents an increase of about 120% with respect to P13 (Figure 15b). This effect is due to the ability of biochar to modify the crack path by increasing the tortuosity and reducing the tip sharpness, so widening the fracture zone. Biochar particles help to increase the toughness of concrete, by improving the microstructure of the material, since they fill the voids and behave as attractors for fracture, so modifying the micro-crack trajectory and making it more tortuous (Figure 12b). This effect makes the concrete able to absorb more energy, especially during unstable fracture. Biochar particles are characterized by a high surface area and demonstrate great compatibility with the cement matrix, as also highlighted by SEM analyses, (Figure 9c). The abovementioned beneficial effects of biochar particles on fracture are indeed known in the literature,[40,59,60] but become even more relevant with the combined use of plastic aggregates. Biochar improves the adhesion of the components in concrete: it is able to fill the additional voids in the cement matrix due to poor compatibility between the plastic grains and the cement matrix, as well as to soak up the water not absorbed by the plastic grains thanks to its high water absorption capability (Figure 12a). The fracture energy of BP13 is indeed 2.5 times greater than that of control (C), which means an increase of about 150%. The increase in residual strength at $CMOD_1 = 0.5$ mm is indeed 197% and 111%, with respect to C and P13 mix, respectively.

5 | CONCLUSIONS

This work investigates the effects of the combined use into concrete of two different waste materials, namely recycled plastic grains and biochar, on mechanical performance. The main findings of this work can be summarized as follows:

1. Workability is strongly influenced by the use of plastic waste and biochar. The substitution of 13% and 20% by volume of aggregates with recycled plastic grains allows reducing the amount of superplasticizer by 50% and 62% respectively to obtain the same flowability as the control batch. Since the effect of biochar addition goes in the opposite direction, in the case of combined use of biochar and plastic grains the required increase of superplasticizer is limited (21%).
2. Density of concrete with natural aggregates partially replaced with recycled plastic grains is reduced up to about 15%; on the contrary, biochar addition has a negligible influence on density.
3. Compressive strength of concrete with natural aggregates partially replaced with recycled plastic grains is strongly reduced due to the poor compatibility between the plastic grains and the cement matrix. The addition of 5% biochar (by weight of cement) helps to reduce the negative effects of plastic on compressive strength, thanks to the filler and water-absorbent properties of biochar particles. Compressive strength is reduced to 27%, 47%, for concrete with 13% and 20% of aggregate replacement, respectively. This reduction is limited to 13% for concrete with 13% of aggregate replacement and 5% of biochar addition.
4. Tensile strength is less influenced than compressive strength by biochar addition and by the replacement of natural aggregates with recycled plastic grains.
5. Tensile post-cracking behavior determined through notched beams subjected to three-point bending, is positively influenced both by the presence of plastics and biochar, resulting in enhanced ductility after cracking onset. Thanks to the ability of plastic grains to slow down the propagation of micro-cracks, fracture energy is increased up to about 30%, 95%, for concrete with 13% and 20% of aggregate replacement, respectively. This percentage is increased to 150% for concrete with 13% of aggregate replacement and 5% of biochar addition. In the same way, also residual strength and ultimate displacement are increased.

The physical and mechanical properties obtained are encouraging and open a path towards the recycling of plastic waste combined with biochar for the development of structural concretes to be used in the building industry. The reduction of density and the beneficial effects on the post-cracking stage offered by plastics and biochar, suggest that this circular concrete can be suitable for several in situ applications, especially in the design of those elements for which weight reduction and ductility are key factors.

ACKNOWLEDGMENTS

This work was financially supported by Emilia Romagna Region in the framework of 2014/20 POR-FESR project "IMPReSA-betonplast: Development of innovative construction materials including non-recyclable plastic particles acting as reinforcement", grant number PG/2018/632099. Authors gratefully acknowledge Ecoplast Srl, Mapei SpA, Cementirossi SpA and Pizzarotti & C. SpA for providing raw materials for specimen preparation.

DATA AVAILABILITY STATEMENT

The data that support the findings of this study are available from the corresponding author upon reasonable request.

ORCID

Patrizia Bernardi https://orcid.org/0000-0003-0554-5870
Beatrice Belletti https://orcid.org/0000-0002-4382-9930

REFERENCES

1. Plastics Europe. Plastics–the facts 2022.
2. Huysman S, De Schaepmeester J, Ragaert K, Dewulf J, De Meester S. Performance indicators for a circular economy: a case study on post-industrial plastic waste. Resour Conserv Recycl. 2017;120:46–54. https://doi.org/10.1016/j.resconrec.2017.01.013
3. Nagy Á, Kuti R. The environmental impact of plastic waste incineration. Acad Appl Res Mil Public Manag Sci. 2016;15:231–7.
4. European Commission, Directorate-General for Research and Innovation. In: De Smet M, Linder M, editor. A circular economy for plastics – Insights from research and innovation to inform policy and funding decisions. Luxemburg: Publications Office of the European Union; 2019. https://data.europa.eu/doi/10.2777/269031.
5. European Commision. A European strategy for plastics in a circular economy, Communication from the Commission to the European Parliament, 2018. https://publications.europa.eu/en/publication-detail/-/publication/e7904416-72a2-11e8-9483-01aa75ed71a1.
6. Poudyal L, Adhikari K. Environmental sustainability in cement industry: an integrated approach for green and economical cement production. Resour Environ Sustain. 2021;4:1–5. https://doi.org/10.1016/j.resenv.2021.100024
7. Mehta KP. Reducing the environmental impact of concrete. Concr Int. 2001;23:61–6.
8. Monteiro PJM, Miller SA, Horvath A. Towards sustainable concrete. Nat Mater. 2017;16:698–9. https://doi.org/10.1038/nmat4930
9. Sandanayake M, Bouras Y, Haigh R, Vrcelj Z. Current sustainable trends of using waste materials in concrete—a decade review. Sustainability. 2020;12:1–38. https://doi.org/10.3390/su12229622

10. Tam VWY, Soomro M, Evangelista ACJ. A review of recycled aggregate in concrete applications (2000–2017). Construct Build Mater. 2018;172:272–92. https://doi.org/10.1016/j.conbuildmat.2018.03.240
11. Nwankwo CO, Bamigboye GO, Davies IEE, Michaels TA. High volume Portland cement replacement: a review. Construct Build Mater. 2020;260:120445. https://doi.org/10.1016/j.conbuildmat.2020.120445
12. Belletti B, Bernardi P, Malcevschi A, Sirico A. Experimental research on mechanical properties of biochar-added cementitious mortars. Proceedings Fib Symposium 2019 Concrete Innovation Materials Design Structure 2019.
13. Akinyemi BA, Adesina A. Recent advancements in the use of biochar for cementitious applications: a review. J Build Eng. 2020;32:101705. https://doi.org/10.1016/j.jobe.2020.101705
14. Chen L, Zhang Y, Wang L, Ruan S, Chen J, Li H, et al. Biochar-augmented carbon-negative concrete. Chem Eng J. 2022; 431:133946. https://doi.org/10.1016/j.cej.2021.133946
15. Gupta S, Kua HW, Low CY. Use of biochar as carbon sequestering additive in cement mortar. Cem Concr Compos. 2018;87: 110–29. https://doi.org/10.1016/j.cemconcomp.2017.12.009
16. Sirico A, Bernardi P, Sciancalepore C, Vecchi F, Malcevschi A, Belletti B, et al. Biochar from wood waste as additive for structural concrete. Construct Build Mater. 2021;303:124500. https://doi.org/10.1016/j.conbuildmat.2021.124500
17. Danish A, Ali Mosaberpanah M, Usama Salim M, Ahmad N, Ahmad F, Ahmad A. Reusing biochar as a filler or cement replacement material in cementitious composites: a review. Construct Build Mater. 2021;300:124295. https://doi.org/10.1016/j.conbuildmat.2021.124295
18. Mensah RA, Shanmugam V, Narayanan S, Razavi SMJ, Ulfberg A, Blanksvärd T, et al. Biochar-added cementitious materials–a review on mechanical, thermal, and environmental properties. Sustainability. 2021;13:1–27. https://doi.org/10.3390/su13169336
19. Qin Y, Pang X, Tan K, Bao T. Evaluation of pervious concrete performance with pulverized biochar as cement replacement. Cem Concr Compos. 2021;119:104022. https://doi.org/10.1016/j.cemconcomp.2021.104022
20. Gupta S, Kua HW. Carbonaceous micro-filler for cement: effect of particle size and dosage of biochar on fresh and hardened properties of cement mortar. Sci Total Environ. 2019;662:952–62. https://doi.org/10.1016/j.scitotenv.2019.01.269
21. Maljaee H, Madadi R, Paiva H, Tarelho L, Ferreira VM. Incorporation of biochar in cementitious materials: a roadmap of biochar selection. Construct Build Mater. 2021;283:122757. https://doi.org/10.1016/j.conbuildmat.2021.122757
22. Gupta S, Kua HW. Effect of water entrainment by pre-soaked biochar particles on strength and permeability of cement mortar. Construct Build Mater. 2018;159:107–25. https://doi.org/10.1016/j.conbuildmat.2017.10.095
23. Ahmad S, Khushnood RA, Jagdale P, Tulliani JM, Ferro GA. High performance self-consolidating cementitious composites by using micro carbonized bamboo particles. Mater Des. 2015; 76:223–9. https://doi.org/10.1016/j.matdes.2015.03.048
24. Ahmad S, Tulliani JM, Ferro GA, Khushnood RA, Restuccia L, Jagdale P. Crack path and fracture surface modifications in cement composites. Frat Integr Strut. 2015;9:524–33. https://doi.org/10.3221/IGF-ESIS.34.58
25. Ferro G, Tulliani JM, Lopez A, Jagdale P. New cementitious composite building material with enhanced toughness. Theor Appl Fract Mech. 2015;76:67–74. https://doi.org/10.1016/j.tafmec.2015.01.005
26. Saikia N, De Brito J. Use of plastic waste as aggregate in cement mortar and concrete preparation: a review. Construct Build Mater. 2012;34:385–401. https://doi.org/10.1016/j.conbuildmat.2012.02.066
27. Gu L, Ozbakkaloglu T. Use of recycled plastics in concrete: a critical review. Waste Manag. 2016;51:19–42. https://doi.org/10.1016/j.wasman.2016.03.005
28. Sharma R, Bansal PP. Use of different forms of waste plastic in concrete–a review. J Clean Prod. 2016;112:473–82. https://doi.org/10.1016/j.jclepro.2015.08.042
29. Alqahtani FK, Zafar I. Plastic-based sustainable synthetic aggregate in green lightweight concrete–a review. Construct Build Mater. 2021;292:123321. https://doi.org/10.1016/j.conbuildmat.2021.123321
30. de Brito J, Agrela F, editors. New trends in eco-efficient and recycled concrete. Duxford, UK: Woodhead Publishing; 2018.
31. Pacheco-Torgal F, Khatib J, Colangelo F, Tuladhar R, editors. Use of recycled plastics in eco-efficient concrete. Duxford, UK: Woodhead Publishing; 2018.
32. EN 1097-6:2013. Tests for mechanical and physical properties of aggregates–Part 6: determination of particle density and water absorption. Brussels, Belgium: CEN; 2013.
33. Tinz J, De Ancos T, Rohn H. Carbon footprint of mechanical recycling of post-industrial plastic waste: Study of ABS, PA66GF30, PC and POM Regrinds. Waste. 2023;1: 127–39.
34. Tan K, Wang J. Substrate modified with biochar improves the hydrothermal properties of green roofs. Environ Res. 2023;216: 114405. https://doi.org/10.1016/j.envres.2022.114405
35. Belletti B, Bernardi P, Fornoni P, Malcevschi A, Sirico A. Development of sustainable cementitious materials by using biochar, Italian Concrete Conference 2022 AICAP/CTE Congress; Naples, Italy, 14–17 April 2021.
36. EN 12390-7:2019, Testing hardened concrete–Part 7: density of hardened concrete. Brussels, Belgium: CEN;2019.
37. ASTM C642-06. Standard test method for density, absorption, and voids in hardened concrete, Annual Book of ASTM Standards. Volume 04.02, ASTM International, 2006.
38. EN 12350-2:2019. Testing fresh concrete–part 2: slump test. Brussels, Belgium: CEN; 2019.
39. EN 206:2013+A1:2016, Concrete–specification, performance, production and conformity. Brussels, Belgium: CEN; 2016.
40. Sirico A, Bernardi P, Belletti B, Malcevschi A, Restuccia L, Ferro GA, et al. Biochar-based cement pastes and mortars with enhanced mechanical properties. Frat Ed Integr Strut. 2020;54: 294–313. https://doi.org/10.3221/IGF-ESIS.54.21
41. EN 12350-6:2019, Testing fresh concrete–Part 6: density. Brussels, Belgium: CEN; 2019.
42. EN 12390-3:2019. Testing hardened concrete–Part 3: compressive strength of test specimens. Brussels, Belgium: CEN; 2019.
43. EN 12390-6:2009, Testing hardened concrete–Part 6: tensile splitting strength of test specimens. Brussels, Belgium: CEN; 2009.

44. JCI-S-001-2003. Method of test for fracture energy of concrete by use of notched beam. Tokyo, Japan: Japan Concrete Institute; 2003.
45. Lobo H, Bonilla JV. Handbook of plastics analysis. New York, NY: CRC Press; 2003. p. 2003.
46. Zarshenas K, Raisi A, Aroujalian A. Surface modification of polyamide composite membranes by corona air plasma for gas separation applications. RSC Adv. 2015;5:19760–72. https://doi.org/10.1039/c4ra15547e
47. Czarnecka-Komorowska D, Wiszumirska K, Garbacz T. Films Ldpe/Lldpe made from post-consumer plastics: processing, structure, mechanical properties. Adv Sci Technol Res J. 2018;12:134–42. https://doi.org/10.12913/22998624/92205
48. Wunderlich B. Crystal nucleation, growth, annealing, macromolecular physics. New York, NY: Academic Press; 1976.
49. Parodi E, Govaert LE, Peters GWM. Glass transition temperature versus structure of polyamide 6: a flash-DSC study. Thermochim Acta. 2017;657:110–22. https://doi.org/10.1016/j.tca.2017.09.021
50. Millot C, Fillot L-A, Lame O, Sotta P, Seguela R. Assessment of polyamide-6 crystallinity by DSC: temperature dependence of the melting enthalpy. J Therm Anal Calorim. 2015;122:307–14. https://doi.org/10.1007/s10973-015-4670-5
51. EN 1992-1-1:2015, Eurocode 2–design of concrete structures–Part 1–1: general rules and rules for buildings. Brussels, Belgium: CEN; 2015.
52. Gupta S, Kua HW, Koh HJ. Application of biochar from food and wood waste as green admixture for cement mortar. Sci Total Environ. 2018;619–620:419–35. https://doi.org/10.1016/j.scitotenv.2017.11.044
53. Praneeth S, Saavedra L, Zeng M, Dubey BK, Sarmah AK. Biochar admixtured lightweight, porous and tougher cement mortars: mechanical, durability and micro computed tomography analysis. Sci Total Environ. 2021;750:142327. https://doi.org/10.1016/j.scitotenv.2020.142327
54. Neville AM. Properties of concrete. London, England: Longman; 1995.
55. Gupta S, Kua HW, Pang SD. Biochar-mortar composite: manufacturing, evaluation of physical properties and economic viability. Construct Build Mater. 2018;167:874–89. https://doi.org/10.1016/j.conbuildmat.2018.02.104
56. Babafemi AJ, Šavija B, Paul SC, Anggraini V. Engineering properties of concrete with waste recycled plastic: a review. Sustainability. 2018;10:3875. https://doi.org/10.3390/su10113875
57. Ohemeng EA, Yalley PP, Dadzie J, Djokoto SD. Utilization of waste low density polyethylene in high strengths concrete pavement blocks production. Civ Environ Res. 2014;6:126–36.
58. Tan K, Qin Y, Wang J. Evaluation of the properties and carbon sequestration potential of biochar-modified pervious concrete. Construct Build Mater. 2022;314:125648. https://doi.org/10.1016/j.conbuildmat.2021.125648
59. Restuccia L, Ferro GA. Promising low cost carbon-based materials to improve strength and toughness in cement composites. Construct Build Mater. 2016;126:1034–43. https://doi.org/10.1016/j.conbuildmat.2016.09.101
60. Sirico A, Belletti B, Bernardi P, Malcevschi A, Pagliari F, Fornoni P, et al. Effects of biochar addition on long-term behavior of concrete. Theor Appl Fract Mech. 2022;122:103626. https://doi.org/10.1016/j.tafmec.2022.103626

AUTHOR BIOGRAPHIES

Alice Sirico, Researcher, Department of Engineering and Architecture (DIA), University of Parma, Parma, Italy

Patrizia Bernardi, Associate Professor, Department of Engineering and Architecture (DIA) & Centre for Energy and Environment-CEE/CIDEA, University of Parma, Parma, Italy

Corrado Sciancalepore, Researcher, Department of Engineering and Architecture (DIA), University of Parma, Parma, Italy

Beatrice Belletti, Full Professor, Department of Engineering and Architecture (DIA) & Centre for Energy and Environment-CEE/CIDEA, University of Parma, Parma, Italy

Daniel Milanese, Full Professor, Department of Engineering and Architecture (DIA), University of Parma, Parma, Italy

Alessio Malcevschi, Researcher, Department of Chemistry, Life Sciences and Environmental Sustainability & Centre for Energy and Environment-CEE/CIDEA, University of Parma, Parma, Italy

How to cite this article: Sirico A, Bernardi P, Sciancalepore C, Belletti B, Milanese D, Malcevschi A. Combined effects of biochar and recycled plastic aggregates on mechanical behavior of concrete. Structural Concrete. 2023;24(5): 6721–37. https://doi.org/10.1002/suco.202200949